

Dalton Transactions

Accepted Manuscript



This article can be cited before page numbers have been issued, to do this please use: M. Bahrami, X. Zhang, M. Ehsani, Y. Jahani and R. M. Laine, *Dalton Trans.*, 2017, DOI: 10.1039/C7DT00373K.



This is an Accepted Manuscript, which has been through the Royal Society of Chemistry peer review process and has been accepted for publication.

Accepted Manuscripts are published online shortly after acceptance, before technical editing, formatting and proof reading. Using this free service, authors can make their results available to the community, in citable form, before we publish the edited article. We will replace this Accepted Manuscript with the edited and formatted Advance Article as soon as it is available.

You can find more information about Accepted Manuscripts in the [author guidelines](#).

Please note that technical editing may introduce minor changes to the text and/or graphics, which may alter content. The journal's standard [Terms & Conditions](#) and the ethical guidelines, outlined in our [author and reviewer resource centre](#), still apply. In no event shall the Royal Society of Chemistry be held responsible for any errors or omissions in this Accepted Manuscript or any consequences arising from the use of any information it contains.

[PhSiO_{1.5}]_{8,10,12} as nanoreactors for non-enzymatic introduction of *ortho*, *meta* or *para*-hydroxyl groups to aromatic molecules.

Mozghan Bahrami,^{1,2} Xingwen Zhang,^{1,3} Morteza Ehsani,² Yousef Jahani,² Richard M. Laine^{1*}

¹Macromolecular Science and Engineering, and Materials Science and Engineering, University of Michigan, Ann Arbor, MI 48109-2136, ²Department of Polymer Processing, Iran Polymer and Petrochemical Institute, 14965/115, Tehran, Iran. ³Department of Chemistry, Harbin Institute of Technology, Harbin 150001, China.

Abstract

Traditional electrophilic bromination follows long established “rules:” electron-withdrawing substituents cause bromination selective for *meta* positions, whereas, electron-donating substituents favor *ortho* and *para* bromination. In contrast, in the [PhSiO_{1.5}]_{8,10,12} silsesquioxanes, the cages act as bulky, electron withdrawing groups equivalent to CF₃; yet bromination under mild conditions, without catalyst, greatly favors *ortho* substitution. Surprisingly, ICl *iodination without catalyst favors* (>90 %) *para* substitution [*p*-IC₆H₄SiO_{1.5}]_{8,10,12}. Finally, nitration and Friedel-Crafts acylation and sulfonylation are highly *meta* selective, > 80 %.

In principle, the two halogenation formats coupled with the traditional electrophilic reactions provide selective functionalization at each position on the aromatic ring. Furthermore, halogenation serves as a starting point for the synthesis of two structural isomers of practical utility, i.e. in drug prospecting. The *o*-bromo and *p*-iodo compounds are easily modified by catalytic cross-coupling to append diverse functional groups. Thereafter, F⁻/H₂O₂ treatment cleaves the Si-C bonds replacing Si with OH. This represents a rare opportunity to introduce hydroxyl groups to aromatic rings, a process not easily accomplished using traditional organic synthesis methods. The as-produced phenol provides additional opportunities for modification. Each cage can be considered a nano-reactor generating 8-12 product molecules. Examples given include syntheses of 4,2'-*R*,*OH*-stilbenes and 4,4'-*R*,*OH*-stilbenes (R = Me, CN). Unoptimized cleavage of the Br/I derivatives yields 55-85% phenol. Unoptimized cleavage of the stilbene derivatives yields 35-40 % (3-5 equivalents of phenol) in the preliminary studies presented here. In contrast, *meta* R-phenol yields are 80 % (7-10 mols per cage).

Introduction

Hydroxylated aromatics (e.g. phenols) are categorized as large-scale commodities, organic intermediates and as important precursors in the pharmaceutical and agrochemical industries.¹⁻¹⁵ However, the introduction of hydroxyl groups to aromatic systems requires a moderately active oxygen species that does not coincidentally destroy the product via total oxidation. A recent publication describes the smooth C-Si bond cleavage of organosilicon compounds with NBS and *m*-CPBA to produce the corresponding *p*-phenols, which complements the work reported here.¹⁶

Hydrogen peroxide has several advantages over other common, low cost oxidants, most of them prepared from hydrogen peroxide itself. The active oxygen content for H₂O₂ exceeds all others save O₃. Further, from an economic perspective the only byproduct is H₂O.¹⁷⁻¹⁹

In commercial practice, Fenton's reagent (Fe³⁺/H₂O₂) is an important tool as it produces extremely reactive hydroxyl radicals often used to treat industrial waste containing toxic organics like benzene, phenol, dyes and pesticides in wastewater, sludges or contaminated soils to reduce toxicity, improve biodegradability and decolorize.²⁰⁻²³ It can also be used for oxyfunctionalization of saturated hydrocarbons to the corresponding alcohols, aldehydes, ketones and carboxylic acids.^{24,25} Despite its numerous advantages, e.g. inexpensive water phase oxidation, its lack of selective oxidation and high oxygen reactivity frequently lead to over oxidation, limiting its synthetic utility.²⁶⁻²⁷

A review of the state-of-the-art in selective hydroxylation of aromatic compounds suggests that oxidative cleavage of the Si-C bonds in [RPhSiO_{1.5}]_{8,10,12} using Fleming-Tamao reagents represents a less explored but potentially quite viable approach to a wide variety of functionalized phenols.

The Fleming-Tamao oxidation of Si-C bonds has been used extensively in the generation of hydroxyl groups at carbon,²⁸⁻³⁵ and is particularly invaluable in natural products syntheses. In general, simple trimethyl and dimethylphenylsilyl groups have been used as “masked” hydroxyl groups. Synthetic routes that employ Fleming-Tamao oxidation as a means of generating substituted phenols are much less well known.^{34,35} Indeed, general and relatively unaggressive methods of generating phenolic compounds seem to be an area that deserves more attention.

Our recent efforts to use F^-/H_2O_2 promoted cleavage of the Si-C bonds in $[RPhSiO_{1.5}]_{8,10,12}$ to form phenols simply to verify substitution patterns on the cage phenyls provided the initial impetus for the current work. Further motivation comes from the fact that *o*-bromination is highly favored in the $[PhSiO_{1.5}]_{8,10,12}$ cages [selectivity is 85 % in $[PhSiO_{1.5}]_8$, 70 % in $[PhSiO_{1.5}]_{10}$ and 60 % in $[PhSiO_{1.5}]_{12}$].^{36,37} This contrasts greatly with iodination with ICl which occurs almost exclusively in the *para* position [90-95 % *para* for all cages].^{38,39} Both of these reactions contrast with traditional nitration and Friedel Crafts acylation and sulfonylation of these cages where substitution at the *meta* position is highly favored [>80 % for all cages].⁴⁰⁻⁴²

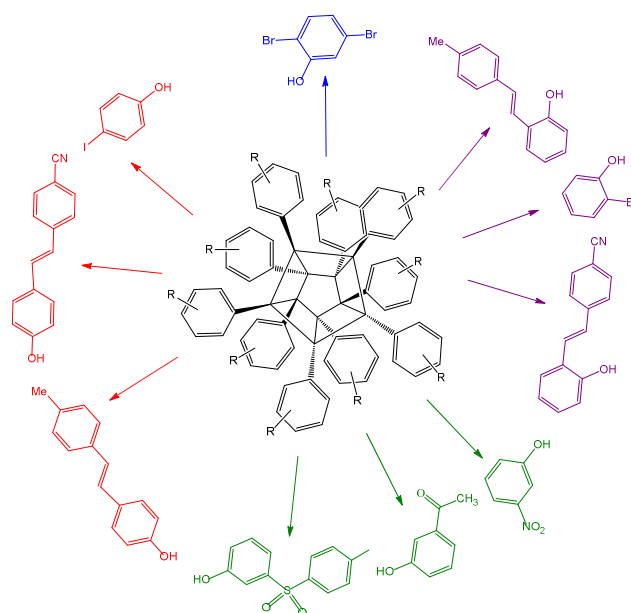
Both *o*-Br and *p*-I compounds are easily functionalized by traditional catalytic cross coupling to introduce the same moieties.⁴³⁻⁴⁵ We are now able to cleave the Si-C bonds in these compounds to introduce hydroxyl groups in the *ortho*, *meta*, or *para* positions as we demonstrate below. Because each $[RPhSiO_{1.5}]_{8,10,12}$ cage will contain 8, 10 or 12 moieties with the same functionality on one cage, F^-/H_2O_2 cleavage will produce multiple examples of the same product, hence the term nanoreactor.

Thus, given that the literature indicates that there are very few, efficient methods of introducing hydroxyl groups to aromatic molecules with the most successful being enzymatic,⁴⁶⁻⁵³ and given the importance that aromatic hydroxyl groups play in drug discovery for example;^{46,47} we

initiated efforts to first understand the mechanism whereby selective *ortho* bromination occurs in the $[\text{PhSiO}_{1.5}]_{8,10,12}$ cages, as discussed recently.^{36,37} The current work represents efforts to show the generality of the cleavage reaction to form phenols with only limited efforts to optimize conversions. These efforts are summarized in Scheme 1.

For perspective purposes, the direct oxidation of benzonitrile to hydroxybenzonitriles was explored using nitrous oxide as oxidant with zeolite catalysts.⁵² Fe free catalysts give $\leq 73\%$ selectivity to hydroxybenzonitriles at benzonitrile conversions of 10%. Three isomers are produced with an o:m:p ratio of 1:6:3.⁵² Although not reported, one presumes that at higher conversions the initial products are further oxidized thereby limiting conversion efficiencies.

In another study, chemically modified graphene (CCG) was used to catalyze the direct oxidation of benzene to phenol using hydrogen peroxide as the oxidant.⁵³ Conversion efficiencies of 18-20 % provided phenol with 98 % selectivities.⁵³ Again, higher conversions were not reported presumably for the same reasons.



Scheme 1. $[\text{RPhSiO}_{1.5}]_{10}$ cage compounds provide access to diverse *ortho*, *meta*, and *para* hydroxylated aromatic compounds and 2,5-dibromophenol in moderate to high yields. (Purple: *Ortho*, Green: *Meta*, Red: *Para*, Blue: difunctional)

Experimental Methods

Materials. The compounds $[\text{PhSiO}_{1.5}]_{8,12}$ and $[m\text{-NitroPhSiO}_{1.5}]_8$ were received as a gift from Mayaterials Inc. $[\text{PhSiO}_{1.5}]_{10}$ was prepared using literature methods.⁵⁴ Bromine, ICl (1.0 M in dichloromethane) and other synthetic reagents were purchased from Sigma Aldrich and used as received. Dichloromethane (CH_2Cl_2) was purchased from Fisher Scientific and distilled from CaH_2 under N_2 prior to use. Dioxane and THF were purchased from Fisher Scientific and distilled from Na/benzophenone under N_2 prior to use.

$[o\text{-BrPhSiO}_{1.5}]_{10}$,³⁶ $[o\text{-BrPhSiO}_{1.5}]_{12}$,³⁶ $[o\text{-BrPhSiO}_{1.5}]_8$,⁵⁵ $[p\text{-IPhSiO}_{1.5}]_{12}$ ³⁹ were synthesized using literature procedures.

General Heck reactions of $[p\text{-IPhSiO}_{1.5}]_{12}$. To a dry 10-mL Schlenk flask under N_2 was added 0.50 g (0.16 mmol, 1.9 mmol-I) of I_{12}DDPS , 19 mg (0.04 mmol) of $\text{Pd}[\text{P}(\text{t-Bu}_3)]_2$, and 18 mg (0.020 mmol) of $\text{Pd}_2(\text{dba})_3$. 1,4-dioxane (3 mL) was then added by syringe, followed by NCy_2Me (3.2 mmol, 0.7 mL) and R-styrene (6.8 mmol). The mixture was stirred at 70°C for 48 h. Then reaction solution quenched by filtering through 1 cm Celite, which was washed with 5 mL THF. The solution was then precipitated into 200 mL methanol and filtered. The solid redissolved in 10 mL THF and filtered again through Celite column to remove any remaining Pd particles, and then precipitated into 200 mL methanol.

General Heck reactions of $[o\text{-BPhSiO}_{1.5}]_8$. To a dry 10-mL Schlenk flask under N_2 was added 0.50 g (0.3 mmol, 2.4 mmol-Br) of $[\text{BrPhSiO}_{1.5}]_8$, 22 mg (0.046 mmol) of $\text{Pd}[\text{P}(\text{t-Bu}_3)]_2$, and 21 mg (0.023 mmol) of $\text{Pd}_2(\text{dba})_3$. 1,4-dioxane (3 mL) was then added by syringe, followed by NCy_2Me (3.7 mmol, 0.8 mL) and R-styrene (8.70 mmol). The mixture was stirred at 70°C for 24 h and then quenched by filtering through 1 cm Celite, which was washed with 5 mL THF. The solution was then precipitated into 200 mL methanol, filtered, and the solid re-dissolved in 10

mL THF. This solution was then filtered again through a 1 cm Celite column to remove any remaining Pd particles, and re-precipitated into 200 mL methanol. Analytical data are presented in the discussion section below.

Removal of residual Pd catalyst. To a dry 50-mL Schlenk flask under N₂ was added 1.0 g of RStyr_xPh₈Si₈O₁₂ dissolved in 10 mL of toluene and 0.1 g of N-acetyl-L-cysteine dissolved in 1 mL of THF. The solution was stirred overnight at room temperature and then filtered through a short silica gel column to remove the insoluble Pd-cysteine complex. The filtrate was then concentrated by rotary evaporation and precipitated into 200 mL of methanol or hexane. The product was filtered and dried in vacuum oven overnight.

[*m*-AcetylPhSiO_{1.5}]₈. To a 250 mL Schlenk flask under N₂, acetyl chloride (19.50 mL, 278.4 mmol) was added into AlCl₃ (20.10 g, 151.2 mmol) in 80 mL of 1:1 (v/v %) ratio of CH₂Cl₂/CS₂ solution. The mixture was stirred at 0° C under N₂ for 15 min. [PhSiO_{1.5}]₈ (10 g, 9.72 mmol, -Ph 80 mmol) was then added to the mixture and the solution was stirred for 5 h at 0° C and then 19 h at room temperature. The reaction was quenched and the organic layer was extracted with 40 mL CH₂Cl₂.

The organic layer was washed with water and then was dried over sodium sulfate, the solvent removed by rotovap and 100 mL CH₂Cl₂ added to the flask. The resulting suspension was filtered. The undissolved powder was dissolved in 100 mL CH₂Cl₂ and passed through the column. Then concentrated by rotovap and precipitated dropwise into 250 mL of hexane, which resulted in a white powder. The powder was collected by filtration, washed with hexane to yield 8 g of the product.

Sulfonylation of [PhSiO_{1.5}]₈. This was a Friedel–Crafts reaction. [PhSiO_{1.5}]₈ (10.34 g, equivalent to 80 mmol of phenyl groups) was suspended in dichloromethane (150 mL) and benzene

sulfonyl chloride (28.32 g, 160 mmol) in a 250-mL, three-necked, round-bottomed flask equipped with a magnetic stirrer and a condenser. AlCl_3 (21.33 g, 160 mmol) was added in three parts over a 10-min period. The mixture was stirred initially at 0°C for a certain time and then allowed to warm to a temperature higher than room temperature for over 2 days. The final solution was poured into ice-water (150 g), and then, a pale yellow precipitate was collected by filtration and washed with n-hexane (500 mL), ethanol (1500 mL), and water (1500 mL) in turn. The resulting solid was then recovered by filtration, redissolved in 50 mL of dichloromethane, filtered through a 1-cm Celite column, reprecipitated into 700 mL of cold ethanol, and vacuum-dried for 8 h. This gave 19.05 g (8.8 mmol, 89% yield) of pale yellow powder.⁴²

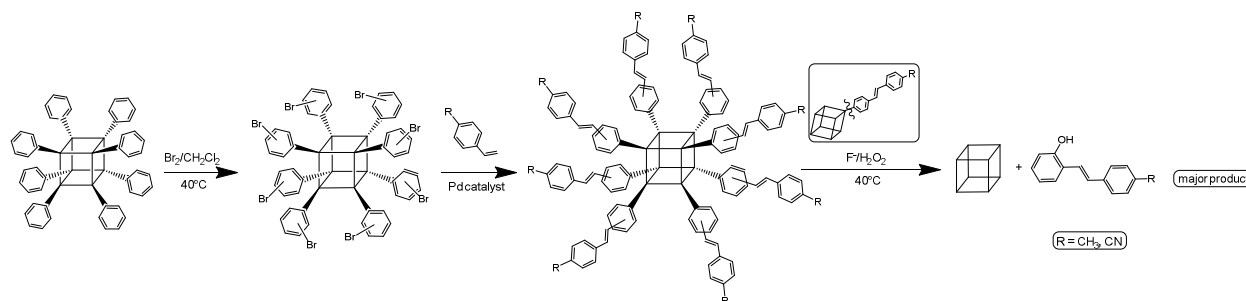
Peroxide Oxidation of Silica Core. A 4.8 g sample of $[\text{BrPhSiO}_{1.5}]_{8/10/12}$, 2.5 g of KF, and 2.0 g of NaHCO_3 were added to a 250 mL round-bottom flask. Then 25 mL of THF was added and the mixture stirred until the silsesquioxane dissolved. Then, 25 mL of methanol and 20 mL of 30% H_2O_2 were added, whereupon the silsesquioxane precipitated. This mixture was then refluxed for 4 h over which time the solution became clear yellow and later precipitated white silica. The solution was then decanted to remove the silica and extracted with ethyl acetate/water three times in order to remove salts. The water layers were combined and extracted with addition ethyl acetate to ensure complete capture of any organic compounds. The combined organic layers were dried over sodium sulfate and evaporated to remove the solvents. The recovered products were analyzed by GC-MS, ^1H NMR, or ^{13}C NMR as discussed above or in SI. The yields for the individual compounds are as follows.

Results and discussion

We recently extended our observation of highly selective *ortho* bromination of $[\text{PhSiO}_{1.5}]_8$ to the larger $[\text{PhSiO}_{1.5}]_{10}$ and $[\text{PhSiO}_{1.5}]_{12}$ cages⁵⁶ to ascertain selectivity differences vs cage size, geometry and electronic ground states as it offers an extreme contrast to ICl promoted iodination which, as noted above, occurs almost exclusively *para* for all cages. In contrast, nitration and Friedel Crafts acylation and sulfonation are highly *meta* selective.⁴⁰⁻⁴² In these previous studies, we found that *ortho* bromination selectivity remains high; albeit, less selective than for $[\text{PhSiO}_{1.5}]_8$ primarily because the phenyl groups sit on the cages at average angles of 72° and 60° partially blocking access to the cage face where interaction with the cage LUMO guides the bromination process.^{36,37}

As discussed in the introduction, the ability to selective *ortho* or *para* halogenate 8 to 12 phenyl groups at once coupled with the ability to further functionalize these cage bound phenyls via catalytic cross-coupling reactions provides routes to quite differently structured organic moieties. The opportunity to effect hydroxylation by $\text{F}^-/\text{H}_2\text{O}_2$ promoted cleavage of the Si-C bonds²⁸⁻³⁵ offers unique utility if it can be developed as a general route to functionalized phenols, potential precursors to pharmaceuticals and/or agrochemicals. This then provides the motivation for the current work.

In the following sections we first briefly discuss efforts to assess *ortho* bromination selectivity in the larger cages which we recently learned to synthesize in high yields as opposed to the traditional $[\text{PhSiO}_{1.5}]_8$.^{36,37} Thereafter, we present studies on $\text{F}^-/\text{H}_2\text{O}_2$ promoted cleavage of $[\text{o-BrPhSiO}_{1.5}]_8$, followed by initial cleavage studies on stilbenes produced via Heck cross coupling reactions with *p*-R-styrene where $\text{R} = \text{Me}$ and CN per Figure 1. Similar studies are presented thereafter for *para* and *meta* derivatives of the PhSQs.



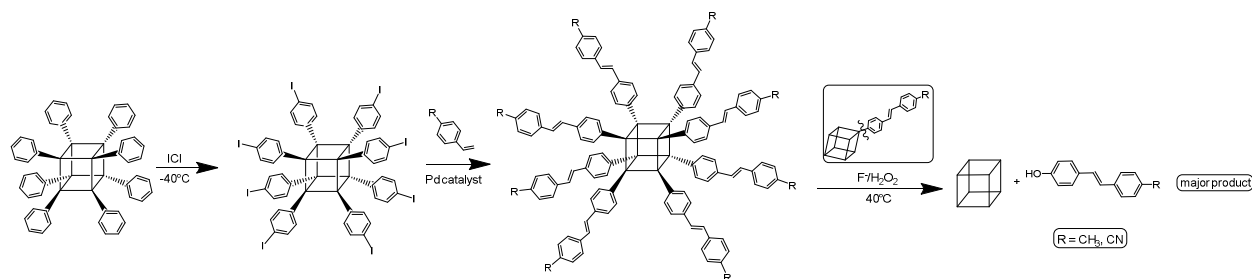


Figure 1. 4,2'-R,OH-stilbene and 4,4'-R,OH-stilbene products using a $[\text{PhSiO}_{1.5}]_{10}$ Nano-reactor.

Synthesis studies. We recently determined that bromination of $[\text{PhSiO}_{1.5}]_{8,10,12}$ without catalyst, at mild temperatures (30–60 °C, see experimental section) provides 60–85 % *ortho* selectivity following recrystallization depending on the cage size as summarized in Table 1.³⁶ This selectivity occurs despite the very bulky nature of the cage attached *ortho* to the bromination site and that these cages exhibit electron withdrawing behavior similar to $-\text{CF}_3$, Table 2.⁵⁷

Table 1 compares selectivity for both *o*-bromination and *p*-iodination using $\text{F}^-/\text{H}_2\text{O}_2$ catalyzed generation of the corresponding phenols. Because we have previously reported the successful functionalization of both types of halogenated cages using multiple catalytic cross coupling reactions,^{34,35} an obvious opportunity arose to produce the corresponding phenols.

Table 1. Bromination of $[\text{PhSiO}_{1.5}]_x$ ($x = 8, 10$ or 12) and $\text{F}^-/\text{H}_2\text{O}_2$ Si-C cleavage[†] products.

characterization SQ	Max in MALDI	Temp. °C	Area % [†] Ortho	% 2- bromophenol ⁴⁷
$[\text{PhSiO}_{1.5}]_8$	$\text{BrPh}_8\text{Si}_8\text{O}_{12}$	30–40	85	~ 90
$[\text{PhSiO}_{1.5}]_{10}$	$\text{Br}_4\text{Ph}_{10}\text{Si}_{10}\text{O}_{15}$	30–40	78	75
$[\text{PhSiO}_{1.5}]_{10}$	$\text{Br}_9\text{Ph}_{10}\text{Si}_{10}\text{O}_{15}$	30–40	75	75
$[\text{PhSiO}_{1.5}]_{12}$	$\text{Br}_6\text{Ph}_{12}\text{Si}_{12}\text{O}_{18}$	40	60	60
$[\text{PhSiO}_{1.5}]_{12}$	$\text{Br}_6\text{Ph}_{12}\text{Si}_{12}\text{O}_{18}$	40	60	60
$[\text{PhSiO}_{1.5}]_{12}$	$\text{Br}_9\text{Ph}_{12}\text{Si}_{12}\text{O}_{18}$	50–55	62	60
$[\text{Br}_2\text{PhSiO}_{1.5}]_8$				90 % 2,5 dibromo phenol
PhSiCl_3	BrPhSiCl_3		5 ^{††}	
$[\text{IPhSiO}_{1.5}]_8$ $[\text{IPhSiO}_{1.5}]_{10}$ $[\text{IPhSiO}_{1.5}]_{12}$				90 % 4-iodophenol

[†]From GC analysis of $\text{F}^-/\text{H}_2\text{O}_2$ cleavage of Phenyl Si-C bond.⁵⁸ ^{††}70 % *meta*, 25 % *para*.⁵⁹

The goal here has been to demonstrate the breadth of this type of hydroxylation rather than to undertake detailed efforts to optimize it. Again, as noted above, one molar equivalent of cage can

Table 2. Ipso ^{13}C for $[\text{PhSiO}_{1.5}]_{8,10,12}$ and $[\text{BrPhSiO}_{1.5}]_{8,10,12}$ and selected model compounds.

Cage	Ipso carbon ^{13}C (ppm)	Cage	Ipso carbon ^{13}C (ppm)
$[\text{PhSiO}_{1.5}]_8$	130.92	$[\text{BrPhSiO}_{1.5}]_8$	129.06
$[\text{PhSiO}_{1.5}]_{10}$	130.55	$[\text{BrPhSiO}_{1.5}]_{10}$	129.01
$[\text{PhSiO}_{1.5}]_{12}$	130.83	$[\text{BrPhSiO}_{1.5}]_{12}$	128.99
$\text{NO}_2\text{C}_6\text{H}_5$	148.30	<i>o</i> - $\text{BrNO}_2\text{C}_6\text{H}_4$	152.80
$\text{CF}_3\text{C}_6\text{H}_5$	130.90	<i>o</i> - $\text{CF}_3\text{BrC}_6\text{H}_4$	130.2 ⁶⁰
$\text{PhSi}(\text{OEt})_3$	131.77	PhSiCl_3	131.55
$[\text{Ph}_2\text{SiO}]_4$	134.42		

produce 8-12 molar equivalents of phenolic products as suggested by Scheme 1 and Tables 3, 6 and 7 below. This aspect suggests that these cages can be termed nanoreactors. This approach appears to offer access to phenolic derivatives not easily generated by any other means as noted in the literature.^{34,35,45-50}

Ortho-functionalized phenols

The first step in these studies was to verify the Table 1 data in more detail. GC-MS analysis for $\text{F}^-/\text{H}_2\text{O}_2$ cleavage of $[\text{BrPhSiO}_{1.5}]_8$ and selected cross-coupling products provides the data presented in Table 3. Three peaks are observed in the GC at retention times (R) = 4.3, 5.4, and 7.1 min, see Table S1 also. The first peak is phenol arising from unsubstituted phenyls and accounts for 30 % of the material in an un-recrystallized sample.

The peaks at R = 5.4 and 7.1 min offer identical mass spectra per Figures S1 and S2. The MS library suggests that they are 3- and 4-bromophenols; however, the published crystal structure of a recrystallized sample shows the compound to be 85 % *ortho* substituted.^{36,37} This is in keeping with the Table 3 GC analyses, which shows one isomer (R = 5.4) integrates to ≈ 92 % of the total area. Having established the identity of the various isomers arising from $\text{F}^-/\text{H}_2\text{O}_2$ cleavage of the starting brominated compounds, the next step was to demonstrate the potential of this approach to generate more sophisticated compounds.

Our objective here was to use a set of well characterized compounds that also offered potential problems with respect to H_2O_2 oxidation. Thus, we previously reported the syntheses of multiple different stilbene derivatives from $[\text{o-BrPhSiO}_{1.5}]_8$ without making any attempt to produce phenol derivatives.^{43,44} In principle, stilbene derivatives may be more difficult to effect $\text{F}^-/\text{H}_2\text{O}_2$ cleavage than other compounds given the exposed double bond. To this end, we chose the rather innocuous *p*-methyl and *p*-cyano derivatives as initial test cases.

Table 3. GC of peroxide cleavage of *o*-functionalized SQs.

Sample	R time (min)	Area %	Formula	MW	m/e (Intensity %)	Assigned Species	Yield %
[<i>o</i> -BrPhSiO _{1.5}] ₈	4.3	30	C ₆ H ₆ O	94	94(100), 66(40), 40(15)	Phenol	
	5.4	53	C ₆ H ₅ BrO	173	173(65), 93(30), 65(100)	Phenol, 2-bromo	
	7.1	17	C ₆ H ₅ BrO	173	173(80), 93(60), 65(100)	Phenol, 4-bromo	
[<i>o</i> -BrPhSiO _{1.5}] ₈ <i>Recrystallized</i>	5.4	92	C ₆ H ₅ BrO	173	173(70), 93(30), 65(100)	Phenol, 2-bromo	45±3
	7.1	8	C ₆ H ₅ BrO	173	173(65), 93(60), 65(100)	Phenol, 4-bromo	
[<i>o</i> -BrPhSiO _{1.5}] ₁₀	5.4	73	C ₆ H ₅ BrO	173	173(90), 93(35), 65(100)	Phenol, 2-bromo	
	7.1	27	C ₆ H ₅ BrO	173	173(75), 93(65), 65(100)	Phenol, 4-bromo	
[<i>o</i> -BrPhSiO _{1.5}] ₁₂	5.4	62	C ₆ H ₅ BrO	173	173(85), 93(35), 65(100)	Phenol, 2-bromo	
	7.1	38	C ₆ H ₅ BrO	173	173(80), 93(60), 65(100)	Phenol, 4-bromo	
[<i>o</i> -MeStyrPhSiO _{1.5}] ₈	10.8	72	C ₁₅ H ₁₄ O	210	210(100), 195(50),	4,2'-Me,OH-stilbene	47±2
	11.3	28	C ₁₅ H ₁₄ O	210	179(30), 210(85)	4,4'-Me,OH-stilbene	
[<i>o</i> -CNStyrPhSiO _{1.5}] ₇ [PhSiO _{1.5}]	4.2	34	C ₆ H ₆ O	94	94(100), 66(55), 40(25)	Phenol	36±3
	11.9	66	C ₁₅ H ₁₁ NO	221	221(100)	4,2'-CN,OH-stilbene	

Mass spectral analysis for F⁻/H₂O₂ cleavage of [*o*-MeStyr₇Ph₈Si₈O₁₂]. The equivalent analyses of the derivatives of the *ortho* brominated cages are as follows. The GC (from GC-MS data) of peroxide cleavage products of [*o*-MeStyr₇Ph₈Si₈O₁₂] also show two peaks (see Table 3) with R = 10.8 and 11.3 min. The peak at R = 10.8 can be identified from the MS library to be 4,2'-Me,OH-stilbene whereas the peak at 11.3 min is 4,4'-Me,OH-stilbene.

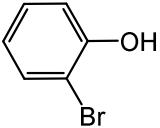
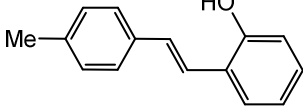
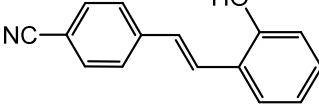
Figures S5 and S6 provide the mass spectral analyses associated with Table 3 data. The *para*-derivative is roughly 30 % of the integrated area and the *ortho* derivative then is approximately 70%. Unfortunately, the separation in the GC is not as clean as observed in Table S1 as might be expected for more polar compounds; consequently, these areas provide only a qualitative measure of the composition. The reader is reminded that these studies were not optimized. Further, note that the selectivities to hydroxylated species are > 65 % out of a 100 % conversion. These results would appear to be superior to the two examples noted above where selectivities were high but conversions quite low.

Mass spectral analysis for F⁻/H₂O₂ cleavage of [*o*-cyanoStyr₇Ph₈Si₈O₁₂]. The analyses for this compound and the resulting peroxide cleaved products are as follow. Figure S7 shows the MALDI of as synthesized [*o*-cyanoStyr₇Ph₈Si₈O₁₂]. The [*o*-cyanoStyrPhSiO_{1.5}]₈ parent ion + Ag is m/z = 2158.

The GC of the peroxide cleavage products shows three peaks at R = 4.2, 7.9 and 12 min. The peak at R = 4.2 is phenol from unsubstituted phenyl and R = 7.9 is ubiquitous in these studies

and arises from butylated hydroxytoluene plasticizer extracted from the rubber septum used to seal the cleavage reaction vials. The remaining broad peak at $R = 12$ min is the target product, see Figure S8 and Table 3. The cleavage gave 66% pure 4,2'-CN,OH-stilbene, while the remainder is phenol from unfunctionalized phenyls.

Table 4. F⁻/H₂O₂ Cleavage yields *o*-phenol compounds for minimum of 3 attempts.

Type	Name	Starting compd mmol	Product Name	Product mmol	Yield %
Ortho	[<i>o</i> -Br ₇ Ph ₈ Si ₈ O ₁₂]	4.4	2-Bromophenol 	2.0	45±3
	[<i>o</i> -Mestyr ₇ Ph ₈ Si ₈ O ₁₂] [<i>o</i> -Br ₇ Ph ₈ Si ₈ O ₁₂]	3.8	4,2'-Me,OH-stilbene 	1.8	47±2
	[<i>o</i> -CyanoStyr ₇ Ph ₈ Si ₈ O ₁₂] [<i>o</i> -Br ₇ Ph ₈ Si ₈ O ₁₂]	3.6	4,2'-CN,OH-stilbene 	1.3	36±3

Para-functionalized phenols

Mass spectral analysis for F⁻/H₂O₂ cleavage of [*p*-IPhSiO_{1.5}]₁₂. Using the cleavage conditions described in the experimental section, we assessed the various products via GC-MS, NMR, FT-IR. Figure S9 shows the MALDI-ToF of the parent [*p*-IPhSiO_{1.5}]₁₂, the data are self-explanatory. It should be noted that [IPhSiO_{1.5}]₁₂ reflects an average of the number of iodinated species present per molecule while MALDI-ToF spectra shows still other species. (*e.g.* I₁₁Ph₁₂Si₁₂O₁₈, I₁₃Ph₁₂Si₁₂O₁₈, *etc.*).

Likewise, the peroxide cleavage products for [*p*-IPhSiO_{1.5}]_{8,10,12} are all essentially identical per Table 1. We present here data for the [PhSiO_{1.5}]₁₂ analog as this nanoreactor provides the most hydroxylated molecules per cage. We see two relevant peaks at $R = 6.4$ and 7.8 min with corresponding integration of 5 and 95 %, Table 5. The mass spectra for both peaks (Figures S10 and S10) are identical and the automated search of the mass spec library identifies these products both as 3-iodophenol.

Table 5 summarizes the mass spec data for all compounds and provides an interpretation of the most intense ions. Introduction of standard 2, 3 and 4-iodophenol samples to the GC-MS shows that the peak at R = 6.4 min is 2-iodophenol and that at 7.8 is the 4-iodophenol as confirmed by ^1H NMR of the isolated cleavage product, Figure S12, as compared with that of an authentic sample in Figure S13. Figure S14 shows the FTIR of the isolated sample and Figure S15 shows the FTIR of the authentic sample.

Mass spectral analysis of *p*-methylstilbene from $[p\text{-MeStyrPhSiO}_{1.5}]_{12}$. As noted just above, the key to the utility of our suggested approach is not just to produce *ortho* and *para* substituted halogenated phenols but to generate more sophisticated derivatives as models of potential efforts to generate *ortho* and *para* phenols in discovery efforts. We recognize that some substituents may not survive peroxide cleavage but given that we have not attempted to optimize the process in any way, the results presented here offer reasonable hope for this new approach.

In general, the yields of the phenolic derivatives: 4,4'-Me,OH-stilbene, 4,2'-Me,OH-stilbene, 4,4'-CN,OH-stilbene and 4,2'-CN,OH-stilbene range from 50 % for the Me compounds to 35-40 % for the CN compounds. This means that the unoptimized yields range from 3-6 molar equivalents of phenol per cage. In principle, the *p*-cyano compounds are most likely to be susceptible to peroxide oxidation given that the electron withdrawing CN groups should aid oxidation of the stilbene on the cage or cleaved phenol product.

The GC trace of peroxide cleaved $[p\text{-MeStyrPhSiO}_{1.5}]_{12}$ (Figures S16 and S17) shows three peaks with residence times recorded in Table 5. The peak at R = 7.9 min is the plasticizer noted above. The peak at R = 10.6 min was identified as the epoxidized 4,4'- Me,OH-stilbene. The peak at R = 11.2 min is 4,4'- Me,OH-stilbene per the mass spec results. As we point out above, one might expect the stilbene double bonds to undergo ready oxidation under the reaction conditions. This likely account for the lower yields than found for the simple halogenated starting materials noted above.

The determination of the R = 7.9 peak comes from the Figure S16 mass spectrum, which has a parent ion at $m/z = 228$, 18 mass units higher than that for the 4,4'- Me,OH-stilbene mass spectrum shown in Figure S17. We presume that this means the initially formed epoxide ring opens thus the added mass is for one water. This peak is just $\approx 1\%$ of the integrated area for the peaks shown. In contrast, the integration for the peak at R = 10.6 min is $\approx 96\%$ of the total area (see Table 5) and offers the mass spectral analysis seen in Table S1.

Based on our identification of the peroxide cleaved product of $[\text{IPhSiO}_{1.5}]_{12}$ as being the *p*-iodophenol, the only product that should form from peroxide cleavage of $[\text{p-MeStyrPhSiO}_{1.5}]_{12}$ would be 4,4'-Me,OH-stilbene. As can be seen, it is by far the major product. The ion intensities of the parent and major ion fragments are presented in Table 5. Note that Tables 3 and 5 represent efforts to demonstrate reproducibility in these studies rather than further optimization.

Table 5. GC of peroxide cleavage of *Para*-functionalized SQs.

Sample	R time (min)	Area %	Formula	MW	m/e (Intensity%)	Assigned species	Yield %
$[\text{p-IPhSiO}_{1.5}]_{12}$	6.4	5	$\text{C}_6\text{H}_5\text{IO}$	220	220(100), 93(40), 65(85)	Phenol, 2-iodo-	
	7.8	95	$\text{C}_6\text{H}_5\text{IO}$	220	220(100), 93(75), 65(65)	Phenol, 4-iodo-	
$[\text{p-IPhSiO}_{1.5}]_{12}$	6.2	2	$\text{C}_6\text{H}_5\text{IO}$	220	220(100), 93(85), 65(35)	Phenol, 2-iodo-	54±2
	7.8	98	$\text{C}_6\text{H}_5\text{IO}$	220	220(100), 93(70), 65(65)	Phenol, 4-iodo-	
$[\text{p-IPhSiO}_{1.5}]_8$	4.5	5	$\text{C}_6\text{H}_6\text{O}$	94	94(100), 66(35), 40(15)	Phenol	57±2
	6.4	3	$\text{C}_6\text{H}_5\text{IO}$	220	220(100), 93(30), 65(55)	Phenol, 2-iodo-	
	7.8	92	$\text{C}_6\text{H}_5\text{IO}$	220	220(100), 93(65), 65(50)	Phenol, 4-iodo-	
$[\text{p-MeStyrPhSiO}_{1.5}]_{12}$	10.6	2	$\text{C}_{15}\text{H}_{16}\text{O}_2$	228	228(100), 178(90)	4,2'-Me,OH-stilbene	44±3
	11.2	98	$\text{C}_{15}\text{H}_{14}\text{O}$	210	210(100), 195(30), 179(20)	4,4'-Me,OH-stilbene	
$[\text{p-MeStyrPhSiO}_{1.5}]_8$ <i>TBAF Cleavage</i>	8.7	12	$\text{C}_{15}\text{H}_{14}$	194	194(85), 179(100), 115(30)	α -methylstilbene	
	9.7	88	$\text{C}_{15}\text{H}_{14}$	194	194(100), 179(100), 115(25)	α -methylstilbene	
$[\text{p-CNStyrPhSiO}_{1.5}]_{12}$	12.5	100	$\text{C}_{15}\text{H}_{11}\text{NO}$	221	221(100)	4,4'-CN,OH-stilbene	

* epoxidized derivative of 4,4'-Me,OH-stilbene

Note that the retention time for the *ortho* derivative is ≈ 0.4 min shorter than for the *para*-phenol as might be anticipated given that the *para* derivative is likely more polar and therefore has a longer residence time in the GC. If we assume that the peroxide cleavage results for the formation of *o*-bromophenol are more likely to be correct then we can suggest that the same ratio (1/99) of 4,2'-Me,OH-stilbene vs 4,4'-Me,OH-stilbene holds in the materials produced here. The mass spectral analyses shown in Figures S16 and S17 are summarized in Table 5. For 4,2'-Me,OH-stilbene, the mass peak shows MW = 228 that is 18 units (H_2O) more than usual MW(210) of 4,2'-Me,OH-stilbene that is due to epoxidation of the double bond followed by ring opening as noted above.

In a separate study, we used nBu_4NF to cleave the Si-C bonds in $[\text{p-Mestyr}_7\text{Ph}_8\text{Si}_8\text{O}_{12}]$ without peroxide to isolate *p*-methylstilbene. Two products are seen in the GC (Table S1) with integration ratios of 12:88 and residence times of 8.7 and 9.7 min, Table 5. The mass spec library

identifies two types of methylstilbenes. We presume that one of these is from regio-selective insertion addition of the Ph-Pd to methylstyrene as expected and produces 88% 1-methyl-4-(2-phenylethenyl) while there is small amount (12%) of the 1,1-addition product as suggested in Figure 2. The mass spectra of both compounds are provided in Figures S18 and S19.

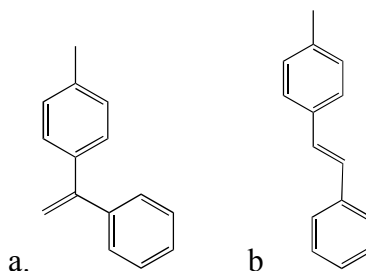


Figure 2. Competitive Heck coupling for methylstilbene a. 1,1-phenyltolylethylene and b. 1-methyl-4-(2-phenylethenyl).

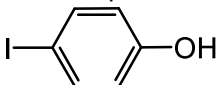
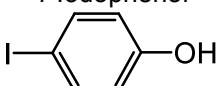
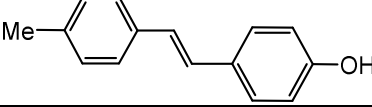
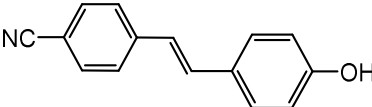
Mass spectral analysis for F^-/H_2O_2 cleavage of $[p\text{-cyanoStyrPhSiO}_{1.5}]_{12}$ The GC of the peroxide cleavage products from $[p\text{-cyanoStyrPhSiO}_{1.5}]_{12}$ (Table S1) shows three peaks at $R = 7.9$, 12.5 and 12.8 min. Table 5 records the integrations and assigned species for some of these peaks and records the mass spec. intensities for the principle ions observed.

The $R = 7.9$ min peak is butylated hydroxytoluene. Both peaks at 12.5 and 12.8 min provide mass spectra (Figures S20 and S21) with similar fragmentation patterns that are not those of the suggested cinnaminonitrile derivative of Figure S22. The width of the peak centered near 12.5 min suggests that the cyano compound is highly polar and moves very poorly in the GC in accord with the difference between the *ortho* and *para* phenols made from the methylstilbene compounds. Again the residence times of the “*ortho*” and “*para*” derivatives as well as the peak shapes support the concept that two different compounds have been made wherein the phenolic group positions differ as anticipated from the peroxide cleavage of the starting halogenated phenyl cages. The GCs of *ortho* and *para* phenol derivatives of cyanostilbene shows that the *R*-time of the *ortho* derivative is ≈ 12 min versus *para*, which is ≈ 12.5 min.

Again, as noted above, the F^-/H_2O_2 cleavage yields for generation of *o*-bromophenol and *p*-iodophenol are typically 55-85 % which equates with 4-5 and 6-7 molar equivalents per mole of cage starting material. The F^-/H_2O_2 cleavage for 4,2'-Me,OH-stilbene and 4,4'-Me,OH-stilbene averages about 50 % which equates to 4 and 6 molar equivalents per mole of cage starting material. In contrast the more easily oxidized 4,2'-CN,OH-stilbene and 4,4'-CN,OH-stilbene F^-/H_2O_2

cleavage product yields average 40 % which equates with 3 and 5 molar equivalents of phenol per cage (Table 6).

Table 6. F⁻/H₂O₂ Cleavage yields *p*-phenol compounds for minimum of 3 attempts.

Type	Name	Starting cmpd mmol	Product Name	Product mmol	% Yield
Para	[<i>p</i> -I ₇ Ph ₈ Si ₈ O ₁₂]	7.3	4-Iodophenol 	4.2	57±2
	[<i>p</i> -I ₁₂ PhSiO _{1.5}] ₁₂	3.9	4-Iodophenol 	2.1	54±2
	[<i>p</i> -Mestyr ₁₂ Ph ₁₂ Si ₁₂ O ₁₈] [<i>p</i> -I ₁₂ Ph ₁₂ Si ₁₂ O ₁₈]	3.8	4,4'-Me,OH-stilbene 	1.8	44±3
	[<i>p</i> -Cyanostyr ₇ Ph ₈ Si ₈ O ₁₂] [<i>p</i> -I ₇ Ph ₈ Si ₈ O ₁₂]	3.6	4,4'-CN,OH-stilbene 	1.5	39±3

Meta-functionalized phenols

As noted above, our objective here is to demonstrate that SQs can act as nanoreactors to produce *ortho*, *para* and *meta* phenol derivatives in acceptable to high yields. Thus, we also synthesized three different *meta* derivatives and characterized them especially with respect to their peroxide cleavage products, anticipating high yields of pure *meta* functionalized phenols.

Mass spectral analysis for F⁻/H₂O₂ cleavage of [*m*-AcetylPhSiO_{1.5}]₈ Thus, we were able to synthesize [*m*-AcetylPhSiO_{1.5}]₈ by Friedel-Crafts acylation of octaphenylsilsesquioxane [PhSiO_{1.5}]₈ with CH₃COCl (Figure 3). This reaction has the highest yields in these series of compounds, and shows just one main GC peak at R = 8.3 min due to 3-hydroxyacetophenone (Table 7). The sample is pure, fully converted and shows no traces of *ortho*, *para* or diacetylated species. ¹H-NMR integration of the acetyl methyl protons using the optimized formylation reaction conditions, has been reported previously, giving a high *meta/para* ratio of > 99:1.⁶¹

Mass spectral analysis for F⁻/H₂O₂ cleavage of [*m*-NitroPhSiO_{1.5}]₈ Analysis of peroxide cleavage of [*m*-NitroPhSiO_{1.5}]₈, (Figure 4) shows three peaks at R = 6.5 and 8.7 min with ratios

of 18, 72 due to *para* and *meta* phenols with ratios of *para/meta* = 25/75. There is a trace at R = 9 min (10%) of dinitro phenol (see Table 7).

Table 7. GC of peroxide cleavage of *Meta*-functionalized SQs.

Sample	R time min	Area %	MW	m/e (Intensity %)	Assigned species	Yield %
[<i>m</i> -AcetylPhSiO _{1.5}] ₈	8.3	100	136	136(65),121(100),93(65),65(45)	3-Hydroxy Acetophenone	76±2
[<i>m</i> -NitroPhSiO _{1.5}] ₈	6.5	18	139	139(100),109(45),81(55),65(80)	Phenol, 2-Nitro	54±3
	8.7	72	139	139(100), 93(20), 65(80)	Phenol, 3-Nitro	
	9	10	184	182(10), 165(75), 89(100), 63(80)	Phenol, DiNitro	
[<i>m</i> -(4-toluene-sulfonyl) PhSiO _{1.5}] ₈	4.8	7	94	94(100), 66(35), 40(15)	Phenol	65±2
	12.8	93	248	248(100),139(100),91(60),65(75)	3-Hydroxy-1-(toluene-4-sulfonyl)benzene	

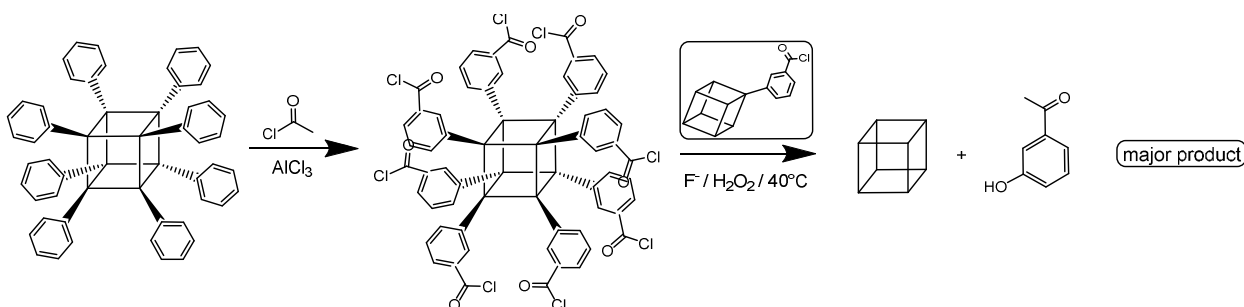


Figure 3. *m*-Hydroxyacetophenone: product of [*m*-AcetylPhSiO_{1.5}]₁₀ Nano-reactor.

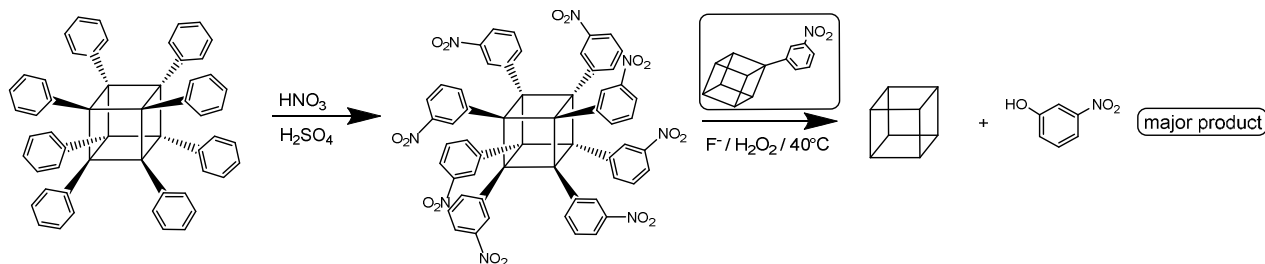


Figure 4. *m*-NitroPhenol: product of [*m*-NitroPhSiO_{1.5}]₁₀ Nano-reactor.

Mass spectral analysis for F⁻/H₂O₂ cleavage of [*m*-(4-toluenesulfonyl)PhSiO_{1.5}]₈. The [*m*-diphenylsulfonylSiO_{1.5}]₈ (ODPSS) was synthesized and characterized previously via one-step Friedel–Crafts reaction in high yield (Figure 5).⁴¹ Using the same procedure, octadiphenylsulfonylsilsesquioxane (ODPSS) was produced and the peroxide cleaved product 3-hydroxy-1-(toluene-4-sulfonyl)-benzene characterized via GC-Mass (Table 7 and Figures S27-S29). A peak in the GC is seen at an R time = 12.6 min and is due to 3-hydroxy-1-(toluene-4-sulfonyl)-

benzene. This is the only sulfonylation product seen, and the substitution is exclusively *meta* (Table 7). The overall yield of the cleavage is 65% and is 93% pure *meta* (Table 8).

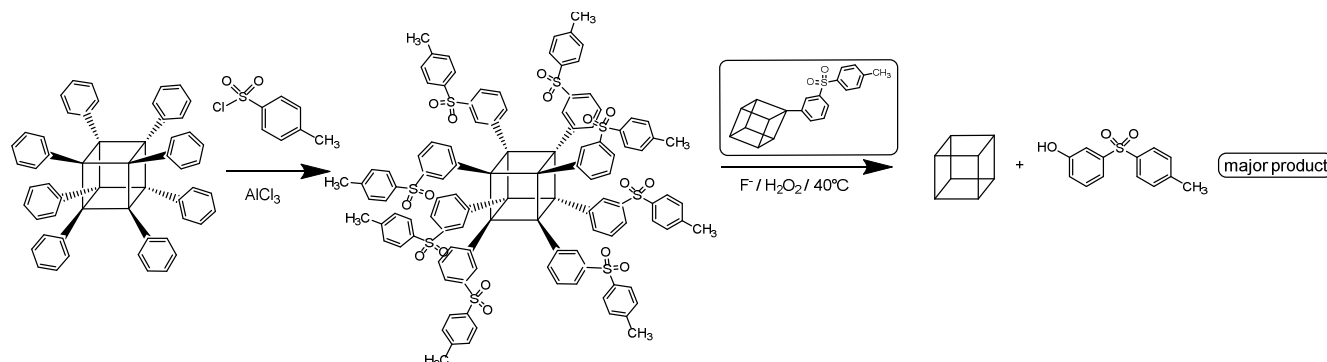


Figure 5. *m*-Hydroxy-1-(toluene-4-sulfonyl)-benzene: product of $[m\text{-diphenylsulfonylSiO}_{1.5}]_{10}$.

Table 8. F^-/H_2O_2 Cleavage yields *m*-phenol compounds for minimum of 3 attempts.

Type	Name	Starting cmpd mmol	Product Name	Product mmol	% Yield
Meta	$[m\text{-NitroPhSiO}_{1.5}]_8$	3.9	3-NitroPhenol 	2.1	54±3
	$[m\text{-AcetylPhSiO}_{1.5}]_8$	3.8	3-Hydroxyacetophenone 	2.9	76±2
	$[m\text{-(4-toluenesulfonyl)PhSiO}_{1.5}]_8$	7.4	3-Hydroxy-1-(toluene-4-sulfonyl)-benzene 	4.8	65±2

Conclusions

The phenyl silsesquioxane cage compounds $[PhSiO_{1.5}]_{8,10,12}$ are unique molecules that exhibit very unusual patterns of electrophilic substitution. Although the $SiO_{1.5}$ unit exhibits electron withdrawing properties equivalent to CF_3 , the halogenation reactions of these cages provide high *ortho* selectivity during bromination with Br_2 and in contrast high *para* selectivity for iodination with ICl . Only in Friedel Crafts acylation and sulfonation with $AlCl_3$ as the catalyst do they exhibit the expected high *meta* selectivity. Furthermore, F^-/H_2O_2 can be used to cleave the phenyl-cage Si-C bonds to generate an OH on the ipso carbon. This represents a rare opportunity to gen-

erate aromatic molecules hydroxylated at either the *ortho* and *para* positions from functionalized $[\text{RPhSiO}_{1.5}]_{8,10,12}$ generated from $[\text{XPhSiO}_{1.5}]_{8,10,12}$ where $\text{X} = o\text{-Br}$ or $p\text{-I}$.

We further briefly explored the potential utility of the $\text{F}^-/\text{H}_2\text{O}_2$ promoted hydroxylation for $[\text{RPhSiO}_{1.5}]_{8,10,12}$ generated from $[\text{XPhSiO}_{1.5}]_{8,10,12}$ where $\text{X} = o\text{-Br}$ or $p\text{-I}$. These efforts focused on using $\text{RPh} = p\text{-methyl}$ or $p\text{-cyanostilbene}$ bound to the silica cage at the 4' or 2' positions. Each cage offers the potential to generate 8, 10 or 12 of the same product molecule hence the appellation "nanoreactor."

In these first unoptimized efforts, we were able to synthesize: (1) 4,2'-Me,OH-stilbene and 4,4'-Me,OH-stilbene and (2) 4,2'-CN,OH-stilbene and 4,4'-CN,OH-stilbene (3) 3-nitrophenol, 3-hydroxy-1-(toluene-4-sulfonyl)-benzene and 3-hydroxyacetophenone in modest to high yields (36-76%). The cyano derivatives, with the highest propensity for oxidation gave the lowest yields. We believe these initial results were sufficiently successful to warrant further efforts to optimize this approach. For example, one might consider running the $\text{F}^-/\text{H}_2\text{O}_2$ promoted hydroxylation using phase transfer catalysis or reducing the reaction temperatures or changing the reaction solvent, or pH. Thus, our work provides potential entrée to a wide variety of complementary hydroxylated aromatics as potential starting points for drug discovery efforts.

Acknowledgements. This work was supported as part of the Center for Solar and Thermal Energy Conversion (CSTEC), an Energy Frontier Research Center funded by the U.S. Department of Energy (DOE), Office of Science, Basic Energy Sciences (BES), under Award # DE-SC0000957. RML would like to thank the Technion, Haifa, Israel for a Lady Davis Fellowship where portions of this manuscript were written. We thank Mr. Joseph Furgal for the ipso carbon NMR data.

Supplementary information

Supplementary information and chemical compound information are available in the online version of the paper. Correspondence and requests for materials should be addressed to RML.

References

1. Halaouli, S., Asther, M., Sigoillot, J. C., Hamdi, M. and Lomascolo, A. "Fungal tyrosinases: New prospects in molecular characteristics, bioengineering and biotechnological applications." *J. Appl. Microbiol.* **2006**, *100*, 219 – 232.
2. Seo, S. Y., Sharma, V. K. and Sharma, N. "Mushroom tyrosinase: Recent prospects." *J. Agric. Food Chem.* **2003**, *51*, 2837 – 2853.
3. Gerdemann, C., Eicken, C. and Krebs, B.; "The crystal structure of catechol oxidase: New insight into the function of Type-3 copper proteins." *Acc. Chem Res.*, **2002**, *35*, 183–191.
4. Sanchez-Ferrer, A.; Rodriguez-Lopez, J. N.; Canovas, F. G. and Carmona, F. G.; "Tyrosinase: A comprehensive review of its mechanism." *Biochim Biophys Acta*, **1995**, *1247*, 1–11.
5. Oksana, S.; Marian, B.; Mahendra, R. and Bo, S. H.; "Plant phenolic compounds for food, pharmaceutical and cosmetics production." *J. Medicinal Plants Res.*, **2012**, *6*, 2526-2539.
6. Georgiou, C. A.; Koupparis, M. A.; "Automated Flow Injection Spectrophotometric Determination of para- and meta-Substituted Phenols of Pharmaceutical Interest Based on Their Oxidative Condensation with 1 -Nitroso-2-naphthol." *Analyst*, **1990**, *115*, 309-313.
7. Bendary, E.; Francis, R.R.; Ali, H.M.G.; Sarwat, M.I.; Hady, S. E.; "Antioxidant and structure–activity relationships (SARs) of some phenolic and anilines compounds." *Annals Agri. Sci.*, **2013**, *58*, 173–181.
8. Rice-Evans, C. A.; Miller, N. J. and Paganga, G.; "Structure-antioxidant activity relationships of flavonoids and phenolic acids." *Free Radical Biology & Medicine*, **1996**, *20*, 933-956.
9. Neyens, E.; Baeyens J.; "A review of classic Fenton's peroxidation as an advanced oxidation technique." *J. Hazardous Mater. B98*, **2003**, *98*, 33–50.
10. Das, T. K.; Wati, M. R.; Shad, K. F.; "Oxidative Stress Gated by Fenton and Haber Weiss Reactions and Its Association With Alzheimer's Disease." *Arch. Neurosci.* **2015**, *2*, e20078, DOI: 10.5812/archneurosci.20078.

11. Pignatello, J. J.; Oliveros, E. and MacKay, A.; "Advanced Oxidation Processes for Organic Contaminant Destruction Based on the Fenton Reaction and Related Chemistry." *Critical Reviews in Environmental Science and Technology*, **2006**, 36, 1–84.
12. Machulek Jr., A.; Quina, F. H.; Gozzi, F.; Silva, V. O.; Friedrich, L. C. and Moraes, J. E. F.; "Fundamental Mechanistic Studies of the Photo-Fenton Reaction for the Degradation of Organic Pollutants." *Organic Pollutants Ten Years after the Stockholm Convention - Environmental and Analytical Update*, **2012**, Chapter 11.
13. Poerschmann, J.; Trommler, U.; Górecki, T.; "Aromatic intermediate formation during oxidative degradation of Bisphenol A by homogeneous sub-stoichiometric Fenton reaction." *Chemosphere*, **2010**, 79, 975–986.
14. Duesterberg, C. K.; Cooper, W. J.; Waite, T. D.; "Fenton-mediated oxidation in the presence and absence of oxygen." *Environ. Sci. Technol.* **2005**, 39, 5052–5058.
15. Duesterberg, C. K.; Mylon, S. E.; Waite, T. D.; "pH effects on iron-catalyzed oxidation using Fenton's reagent." *Environ. Sci. Technol.* **2008**, 42, 8522–8527.
16. Hosomi, A.; Iijima, S. and Sakurai H. "Carbon-silicon bond cleavage of organotrialkoxysilanes and organosilatrane with *m*-chloroperbenzoic acid and *n*-bromosuccinimide. new route to phenols, primary alcohols and bromides" *Chemistry letters*, **1981**, 243–246.
17. Strukul, G.; "Catalytic oxidations with hydrogen peroxide as oxidant." *Catal. by Metal Complexes*, Volume 9, **1992**.
18. Jones, C. W.; "Applications of Hydrogen Peroxide and Derivatives." **1999**.
19. Kaczorowska, K.; Kolarska, Z.; Mitka, K. and Kowalski, P.; "Oxidation of sulfides to sulfoxides. Part 2: Oxidation by hydrogen peroxide." *Tetrahedron*, **2005**, 61, 8315–8327.
20. Mohajeri, S.; Aziz, H. A.; Isa, M. H.; Bashir, M. J.; Mohajeri, L. and Adlan, M. N.; "Influence of Fenton reagent oxidation on mineralization and decolorization of municipal landfill leachate." *J. Environmental Sci. and Health A*, **2010**, 45, 692–698.
21. Lucas, M. S.; Peres, J. A.; "Removal of COD from olive mill waste water by Fenton's reagent: Kinetic study." *J. Hazardous Mater.*, **2009**, 168, 1253–1259.
22. Kitis, M.; Adams, C. D. and Daigger, G. T.; "The effects of Fenton's reagent pretreatment on the biodegradability of nonionic surfactants." *Water Res.* **1999**, 33, 2561–2568.

23. Ventura, A.; Jacquet, G.; Bermond, A.; Camel, V.; "Electrochemical generation of the Fenton's reagent: application to atrazine degradation." *Water Res.*, **2002**, *36*, 3517–3522.
24. Gozzo, F.; "Radical and non-radical chemistry of the Fenton like systems in the presence of organic substrates." *J. Molecular Catalysis A: Chemical*, **2001**, *171*, 1–22.
25. Shi, F.; Tse, M. K.; Li, Z. and Beller, M.; "Controlling iron catalyzed oxidation reactions: from non-selective radical to selective non-radical reactions." *Chemistry*, **2008**, *14*, 8793–8797.
26. Laat, J.; Le, T. G.; "Effects of chloride ions on the iron(III)-catalyzed decomposition of hydrogen peroxide and on the efficiency of the Fenton-like oxidation process." *Applied Cat. B: Environmental*, **2006**, *66*, 137–146.
27. Haber, F. and Weiss, J.; "The catalytic decomposition of hydrogen peroxide by iron salts." *Proc. Royal Soc. A*, **1934**, *147*, 332–351.
28. Tamao, K.; Kumada, M.; Maeda, K. "Silafunctional compounds in organic synthesis 21. Hydrogen peroxide oxidation of alkyenyl(alkoxy)silanes," *Tetrahedron Lett.*, **1984**, *25*, 321–324.
29. Tamao, K. and Ishida, N. "Silafunctional compounds in organic synthesis XXVI. Silyl groups synthetically equivalent to the hydroxy group," *J. Organometallic Chem.*, **1984**, *269* C37–C39.
30. Jones, G. R. and Landais, Y. "The Oxidation of the Carbon-Silicon Bond," *Tetrahedron*, **1996**, *52*, 7599–7662.
31. Fleming, I.; Barbero, A.; Walter, D. "Stereochemical Control in Organic Synthesis Using Silicon-Containing Compounds," *Chem Rev.*, **1997**, *97*, 2063–2192.
32. Barrett, A. G. M.; Head, J.; Smith, M. L.; Stock, N. S.; White, A. J. P.; Williams, D. J.; "Fleming–Tamao Oxidation and Masked Hydroxyl Functionality: Total Synthesis of (+)-Pramanicin and Structural Elucidation of the Antifungal Natural Product (–)-Pramanicin," *J. Org. Chem.*, **1999**, *64*, 6005–6018
33. Chiara, J. L.; García, Á.; Sesmilo, E.; Vacas, T.; "1-Silyl-2,6-diketones: Versatile Intermediates for the Divergent Synthesis of Five- and Six-Membered Carbocycles under Radical and Anionic Conditions," *Org. Lett.*, **2006**, *8*, 3935–3938.
34. Simmons, E. M. and Hartwig, J. F. "Iridium-Catalyzed Arene Ortho-Silylation by Formal Hydroxyl-Directed C-H Activation," *J. Am. Chem. Soc.* **2010**, *132*, 17092–17095.

35. Rayment, E. J.; Summerhill, N.; Anderson, E. A. "Synthesis of Phenols via Fluoride-free Oxidation of Arylsilanes and Arylmethoxysilanes," *J. Org. Chem.*, **2012**, 77, 7052–7060.
36. Bahrami, M.; Kieffer, J.; Hashemi, H.; Ma, X. and Laine, R. M. "Why do the $[\text{PhSiO}_{1.5}]_{8,10,12}$ cages self-brominate primarily in the ortho position? Modeling reveals a strong cage influence on the mechanism." *Phys. Chem. Chem. Phys.*, **2014**, 16, 25760-25764.
37. Bahrami, M.; Furgal, J. C.; Hashemi, H.; Ehsani, M.; Jahani, Y.; Goodson III, T.; Kieffer, J. and Laine, R. M. "Synthesis and Characterization of Nano-building Blocks $[o\text{-RStyrPhSiO}_{1.5}]_{10,12}$ (R = Me-, MeO-, NBoc- and CN. Unexpected Photophysical Properties Arising from Apparent Asymmetric Cage Functionalization as Supported by Modelling Studies," *J. Phys. Chem. C*. DOI: 10.1021/acs.jpcc.5b02678
38. Roll, M. F.; Asuncion, M. Z.; Kampf, J.; and Laine, R. M.; "Para-Octaiodophenylsilsesquioxane, $[p\text{-IC}_6\text{H}_4\text{SiO}_{1.5}]_8$, a Nearly Perfect Nano-Building Block." *ACS Nano*, **2008**, 2, 320–326.
39. Roll, M. F.; Kampf, J. W.; Kim, Y.; Yi, E.; Laine, R.M.; "Nano-Building Blocks via Iodination of $[\text{PhSiO}_{1.5}]_n$ forming $[p\text{-I-C}_6\text{H}_4\text{SiO}_{1.5}]_n$ where $n = 8, 10, 12$ and a new route to high surface area, thermally stable, microporous materials via thermal elimination of I_2 ." *J. Am. Chem. Soc.* **2010**, 132, 10171–10183.
40. Kim, S.G.; Choi, J.; Tamaki, R.; Laine, R. M.; "Synthesis of amino-containing oligophenylsilsesquioxanes." *Polymer*, **2005**, 46, 4514–4524.
41. Brick, C.; "Functionalization of Phenylsilsesquioxane." Ph.D. Dissertation, University of Michigan, **2005**.
42. Li, Z.; Yang. R.; "Synthesis, Characterization and Properties of a Polyhedral Oligomeric Octadiphenylsulfonylsilsesquioxane," *J. Appl. Polymer Sci.*, **2014**, 131, 40892.
43. Sulaiman, S.; Zhang, J.; Goodson, III, T.; Laine, R. M. "Synthesis, Characterization and Photophysical Properties of Polyfunctional Phenylsilsesquioxanes: $[o\text{-RPhSiO}_{1.5}]_8$, $[2,5\text{-R}_2\text{PhSiO}_{1.5}]_8$, and $[\text{R}_3\text{PhSiO}_{1.5}]_8$." *J. Mater. Chem.* **2011**, 21, 11177-11187.
44. Laine, R. M.; Sulaiman, S.; Brick, C.; Roll, M.; Tamaki, R.; Asuncion, M. Z.; Neurock, M.; Filhol, J. S.; Lee, C.Y.; Zhang, J.; Goodson III, T.; Ronchi M.; Pizzotti, M.; Rand, S. C.; Li, Y. "Synthesis and photophysical properties of stilbene octasilsesquioxanes. Emission behavior coupled with theoretical modeling studies suggest a 3-D excited state involving the silica core." *J. Am. Chem. Soc.* **2010**, 132, 3708–3722.

45. Laine, R. M. and Roll, M. F. "Polyhedral Phenyl silsesquioxanes" *Macromolecules*, **2011**, *44*, 1073-1109 and references therein.
46. a. Koerts, J.; Velraeds, M. M. C.; Soffers, A. E. M. F.; Vervoort, J.; Rietjens, I. M. C. M.; "Influence of Substituents in Fluorobenzene Derivatives on the Cytochrome P450-Catalyzed Hydroxylation at the Adjacent Ortho Aromatic Carbon Center." *Chem. Res. Toxicol.* **1997**, *10*, 279-288. b. Sarabia, S. F.; Zhu, B. T.; Kurosa, T.; "Mechanism of Cytochrome P450-Catalyzed Aromatic Hydroxylation of Estrogens." *Chem. Res. Toxicol.* **1997**, *10*, 767-771.
47. a. Mitoma, C.; Posner, H. S.; Reitz, H. C. and Udenfriend, S.; "Enzymatic Hydroxylation of Aromatic Compounds." *Arch. Biochem. And Biophys.* **1956**, *61*, 431-441. b. Ullrich, R. and Hofrichter, M., "Enzymatic hydroxylation of aromatic compounds." *Cell. Mol. Life Sci.* **2007**, *64*, 271 – 293 and references therein.
48. a. Lücke, B.; Narayana, K.V.; Martin, A. and Jähnisch, K., "Oxidation and ammoxidation of aromatics." *Adv. Synth. Catal.* **2004**, *346*, 1407-1424. b. Mukherjee, P.; Bhaumik, A.; Kumar, R. "Eco-friendly, Selective Hydroxylation of C-7 Aromatic Compounds Catalyzed by TS-1/H₂O₂ System under Solvent-free Solid-Liquid-Liquid-Type Triphase Conditions." *Ind. Eng. Chem. Res.* **2007**, *46*, 8657-8664.
49. Tani, M.; Sakamoto, T.; Mita, S.; Sakaguchi, S. and Ishii, Y.; "Hydroxylation of benzene to phenol under air and carbon monoxide catalyzed by molybdovanadophosphoric acid." *Angew. Chem. Int. Ed. Engl.* **2005**, *44*, 2586-2588.
50. Hamilton, G. A.; Hanifin Jr., J. W.; Friedman, J. P.; "The Hydroxylation of Aromatic Compounds by Hydrogen Peroxide in the Presence of Catalytic Amounts of Ferric Ion and Catechol. Product Studies, Mechanism and Relation to Some Enzymic Reaction." *J. Am. Chem. Soc.*, **1966**, *88*, 5269-5272.
51. Hamilton, G. A.; Friedman, J. P.; Campbell, P. "The Hydroxylation of Anisole by Hydrogen Peroxide in the Presence of Catalytic Amounts of Ferric Ion and Catechol. Scope, Requirements, and Kinetic Studies." *J. Am. Chem. Soc.*, **1966**, *88*, 5266-5268.
52. Ehrich, H.; Schwieger, W.; Jähnisch, K.; "Investigations on the selective oxidation of benzonitrile using nitrous oxide catalyzed by modified ZSM-5 zeolites." *Applied Catalysis A: General*, **2004**, *272*, 311–319.

53. Yang, J.; Sun, G.; Gao, Y.; Zhao, H.; Tang, P.; Tan, J.; Lub, A. and Ma, D.; "Direct catalytic oxidation of benzene to phenol over metal-free graphene-based catalyst." *Energy Environ. Sci.*, **2013**, *6*, 793–798.
54. a. Ossadnik, C.; Veprek, S.; Marsmann, H.C.; Rikowski, E. "Photolumineszenzeigenschaften von substituierten Silsesquioxanen der Zusammensetzung $R_n(\text{SiO}_{1.5})_n$," *Monat. für Chem.* **1999**, *130*, 55-68. b. Azinovic, D.; Cai, J.; Eggs, C.; König, H.; Marsmann, H.C.; Veprek, S. "Photoluminescence from silsesquioxanes $R_8(\text{SiO}_{1.5})_8$," *J. Luminescence*, **2002**, *97*, 40-50.
55. Roll, M.F.; Mathur, P.; Takahashi, K.; Kampf, J. W.; Laine, R. M. "[PhSiO_{1.5}]₈ promotes self-bromination to produce [o-BrPhSiO_{1.5}]₈: further bromination gives crystalline [2,5-Br₂PhSiO_{1.5}]₈ with a density of 2.32 g cm⁻³ and a calculated refractive index of 1.7 or the tetraicosa bromo compound [Br₃PhSiO_{1.5}]₈" *J. Mater. Chem.*, **2011**, *21*, 11167-11176.
56. J. C. Furgal, T. Goodson III, R. M. Laine, "D5h [PhSiO_{1.5}]₁₀ synthesis via F⁻ catalyzed rearrangement of [PhSiO_{1.5}]_n. An experimental/computational analysis of likely reaction pathways, *Dalton Trans.*, **2016**, *45*, 1025.
57. Feher, F.J.; Budzichowski, T.A. "Syntheses of highly-functionalized polyhedral oligosilsesquioxanes." *J. Organometallic Chem.*, **1989**, *379*, 33-40.
58. Brick, C.M. Tamaki, R.; Kim, S.-G.; Asuncion, M.Z.; Roll, M.; Nemoto, T.; Ouchi, Y.; Chujo Y.; Laine, R.M. "Spherical, Polyfunctional Molecules Using Poly(bromophenylsilsesquioxane)s as Nanoconstruction Sites." *Macromolecules*, **2005**, *38*, 4655-4660.
59. Private Communication, Dr. S. Sulaiman, Gelest Inc. Gelest Product SIB1903.0
60. Newmark, R. A.; Hill, J. R. "Carbon-13–fluorine-19 coupling constants in benzotrifluorides," *Org. Mag. Res.* **1977**, *9*, 589-592.
61. Kawakami, Y.; Kabe Y.; "Novel meta-Selective Friedel-Crafts Acylation of Phenylsilsesquioxane." *Chem. Lett.* **2010**, *39*, 1082-1083.